Verification Firings of End-burning Type Hybrid Rockets

Harunori Nagata[1], Hayato Teraki[2], Yuji Saito[3], Ryuichiro Kanai[4]
Hokkaido University, Sapporo 060-8628, Japan

Hiroyuki Yasukochi[5]
The University of Tokyo, Tokyo 113-0033, Japan

Masashi Wakita[6], Tsuyoshi Totani[7]
Hokkaido University, Sapporo 060-8628, Japan

The authors have previously proposed the concept of end burning type hybrid rockets which would use cylindrical fuel grains consisting of an array of many small ports running in the axial direction through which oxidizer gas would flow. Because of difficulty in manufacturing a fuel grain that satisfied requirements such as high volumetric filling rate (above 0.95) and micro-sized port intervals, the end burning hybrid rocket had yet to be achieved. This paper reports the results of verification firing tests of a novel end burning type hybrid rocket made possible for the first time by recent progress in 3D printing technology. The results clearly distinguish the initial transient and steady periods of the end burning mode, and prove that no oxidizer to fuel ratio shift occurs during firing. Since the initial transient is a period for the exit end face to attain a steady state shape, an initial end face shape being close to the steady state shape can shorten this period. A firing test with fuel having tapered ports is shown to attain a steady state shape in less than 1 second, which is much shorter than the non-tapered case of about 6 seconds.

I. Introduction

FOR its advantages such as safety and low cost, hybrid rockets have attracted attention of rocket engineers since

[1] Professor, Faculty of Engineering, Hokkaido University, Sapporo 060-8628, Japan, AIAA Member.
[2] Master's course student, Graduate School of Engineering, Hokkaido University, Sapporo 060-8628, Japan.
[3] Master's course student, Graduate School of Engineering, Hokkaido University, Sapporo 060-8628, Japan.
[4] Doctor's course student, Graduate School of Engineering, Hokkaido University, Sapporo 060-8628, Japan.
[5] Specially-appointed researcher, Institute for Photon Science and Technology, The University of Tokyo, Tokyo 113-0033, Japan.
[6] Assistant professor, Faculty of Engineering, Hokkaido University, Sapporo 060-8628, Japan.
[7] Associate professor, Faculty of Engineering, Hokkaido University, Sapporo 060-8628, Japan.

the dawn of rocket propulsion concept. Actual hybrid rockets developed up to now, however, exhibit definitive weak points: low combustion efficiency and O/F (oxidizer to fuel ratio) shift during firing and throttling. The low combustion efficiency results from poor mixing between oxidizer and fuel in a turbulent boundary layer over a fuel surface. Although throttleability is a virtue of hybrid rockets, O/F shift accompanies throttling, resulting in the loss of specific impulse. Even without any throttling, O/F shift occurs due to a change in burning surface area during firing. To overcome these defects, the authors have proposed the concept of an end burning type hybrid rocket [1-4]. Figure 1 outlines the basic idea behind the end burning type hybrid rocket concept. A key point of this idea is that a motor uses a cylindrical fuel grain incorporating an array of many small ports running in the axial direction through which oxidizer gas flows. A diffusion flame stabilizes at each port exit. Higher combustion efficiency can be expected because each flame has a sufficient mixing area; an envelope flame appears immediately above the exit end face as if premixed gas were blowing from the burning surface. Just after ignition, the burning surface area changes with time due to a micro-flame at each port exit propagating upstream. Since each port exit expands with time, neighboring ports eventually merge with one other, as shown in Fig. 2. After this initial transient, no O/F shift occurs during firing because the burning surface area no longer changes. Our previous research [5] has revealed that the burning rate (or the flame traveling velocity) in the axial direction depends on pressure, and that the pressure exponent is close to unity (around 0.95). This means virtually no O/F shift during throttling.

To realize an end-burning mode, it is necessary to prevent a flame spreading upstream in a port and to maintain the position of the envelope flame at the exit surface. A basic study using a single port fuel [6-8] has clarified that the Damkohler numbers in ports should exceed a certain value for this purpose. We made a trial design for verification test firings and found that the volumetric filling rate of a fuel must exceed 0.953. The number of ports should be large as possible because the initial transient duration gets longer with increasing port intervals. To fulfill these two requirements, many small diameter ports are necessary. After reaching this conclusion, we gave up verification tests because of the inability to manufacture a fuel grain of this shape. Recently, Li et al. [9] reported an end-burning mode obtained in static firing tests with an axial-injection end-burning hybrid rocket motor. However, their understanding of "end-burning" is different from our original idea; the opposed propagating mode in their observation corresponds to our end burning mode. The end-burning mode in their paper does not have the virtues expected of our end burning hybrid rockets such as outstanding throttling characteristic, high axial regression rate, and high combustion efficiency. Since the number of ports was too small and the port interval was too large, their

opposed propagating mode, corresponding to our original idea, could not reach a steady state. Accordingly, the end burning hybrid rocket has yet to be achieved due to the tough requirements of high volumetric filling rate and small port intervals. However, recent progress in 3D printing technology has opened up new opportunities for high-precision manufacturing; we can make any shape of solid fuel now, and with the precision required to realize the end burning hybrid rocket concept. This paper reports results of verification firing tests of an innovative new end burning type hybrid rocket made possible only by the advent of high precision 3D printing technology.

II. Fuel Grain and Test Motor

Figure 3 shows a fuel grain made by a high precision light polymerized 3D printer. It is an ultraviolet curable resin consisting of 80 to 90% acrylic acid ester, 5% hexamethylene acrylate, and photopolymerization initiator. The diameter and length of the fuel grain are 20 mm and 50 mm, respectively. This is around the maximum size we can produce in an acceptable yield rate by the current technology level. Improving the stability of the 3D printer is necessary to increase the size because the yield rate decreases with increasing the number of layers. The inner diameter of each port is 0.3 mm with an error of plus or minus 0.01 mm and the spacing between ports is 2.0 mm. As a result, a high volumetric filling rate of 98.1% comes out. Figure 4 shows a schematic view of the test motor. Gaseous oxygen (GOX in the figure) flows into the combustion chamber from the left, and enters the fuel grain from the left end face. The nozzle is a sonic type with an inner diameter of 2.5 mm. An electrically heated nichrome wire at the exit end surface ignites the fuel. After a prescribed firing duration, nitrogen gas purges the combustion chamber to stop firing quickly. The main measurements made during firing are combustion chamber pressure and oxygen flow rate. After a firing test, residual fuel grain is recovered from the combustion chamber for measure and weigh-in, as well as careful observation of regression characteristics. Table 1 summarizes the conditions of the six firing tests conducted in this study. Pressure measurements were taken with a Kyowa PHB-A-20MPa pressure sensor rated to plus/minus 0.08 [MPa] in accuracy. Oxygen flow rate was measured with an Azbil CMS0200 flowmeter rated to plus/minus 3%. Initial and final fuel mass was measured using an A&D FX-300i digital scale rated to plus/minus 0.001 [g]. In Test-05 and Test-06, port exits were tapered. The details of the taper will be described in the next section.

III. Results and Discussion

Figures 5 and 6 shows histories of chamber pressure and oxygen flow rate obtained in all tests listed in Table 1. Pressures are shown in absolute pressure values. In Test-01 and Test-02 pressure oscillations are observed. These oscillations are due to the inaccuracy in the 3D-printing. After Test-03 the stability of the 3D printer was improved and this problem was resolved. In Test-02 the flame entered into a port at 4.5 [s] and subsequently spread upstream, resulting in a sudden pressure increase. In all pressure histories chamber pressure keeps almost a constant value after an initial transient. This result represents that it attains a steady end burning mode after an initial transient. Note that the duration of the initial transient in Test-04 is around 5 to 6 seconds. Figure 7 shows the fuel grain used in Test-04 before and after firing. The exit end face view clearly shows that neighboring ports are tangent to one other. In the side view, the burning end face after firing is almost flat, showing that the end-burning mode was achieved. The mean axial regression distance calculated from the mass difference between before and after firing was 13.2 mm.

To obtain the O/F history during firing, we adopted a reconstruction technique [10]. The reconstruction technique calculates temporal O/F by solving the following equation:

(1)

where η, c^*_{th}, p_c , A_t , and $\dot{m}_o$ are c^* efficiency, theoretical c^*, chamber pressure, nozzle throat area, and oxygen flow rate, respectively. The c^* efficiency η was adjusted so that the calculated total fuel mass consumption agrees with the experimentally measured value. Figure 8 shows the result of reconstructed O/F and fuel flow rate histories in Test-04 with plus/minus error. This error was determined by analyzing the bias introduced from experimental measurements. The overall uncertainty in the reconstructed O/F, $B_{\mathrm{O/F}}(t)$, is calculated from the following equation:

$$B_{\mathrm{O/F}}(t)=\sqrt{\left(\frac{\partial \mathrm{O/F}(t)}{\partial\, p_c(t)}B_{p_c}\right)^2+\left(\frac{\partial \mathrm{O/F}(t)}{\partial \dot{m}_o(t)}B_{\dot{m}_o(t)}\right)^2+\left(\frac{\partial \mathrm{O/F}(t)}{\partial M_f}B_{M_f}\right)^2} \tag{2}$$

where M_f is the total fuel mass consumption and B_{p_c}, $B_{\dot{m}_o(t)}$, and B_{M_f} are measurement uncertainties of chamber pressure, oxygen flow rate, and total fuel mass consumption, respectively. During the ignition transient, fuel flow rate decreases with time before leveling off, after which stays almost constant for the rest of firing. This result verifies that no O/F shift occurred during firing, and thus the virtue of constant O/F operation underlying the original end burning hybrid rocket concept was realized.

Assuming a flat regression in axial direction, the fuel flow rate history gives the histories of axial regression rate and regression distance, as shown in Fig. 9 with plus/minus error. Because the total mass consumption is used as an input data in the reconstruction technique, the error in the regression distance decreases with time. The initial transient duration depends on the port spacing. Since the port spacing is 2 mm and each port diameter is 0.3 mm, neighboring ports merge with one another when the radial regression distance reaches 0.85 mm. A previous study [5] revealed that the relationship between radial and axial regression in each port shows a weak dependence on the port diameter, as seen in Fig. 10. According to this result, the initial transition period ends when the axial regression distance reaches 7 to 8 mm. This means that the duration of the initial transient is slightly more than 5 seconds, as Fig. 11 shows. The initial transient of slightly more than 5 seconds is consistent with the pressure history in Fig. 5 and the fuel flow rate history in Fig. 8.

Another virtue of end burning type hybrid rockets is a remarkable throttling characteristic; O/F shows almost no variation during throttling. To investigate the effect of throttling, i.e., oxidizer flow rate, on O/F, we conducted several firing tests with various oxidizer flow rates. Figure 12 shows the results of these tests. The error bars in the figure come from the precision limit of port diameters, which is plus or minus 0.01 mm for the design value of 0.3 mm. Our previous study has revealed that 1% error in port area results in about 3% error in O/F [5]. This means that the 0.01 mm error in the inner diameter causes about 20% error in O/F. As a result, each plot in the figure lies between error bars of other plots and it shows no clear trend on the effect of oxidizer flow rate on O/F. To show the remarkable throttling characteristic more clearly, we have to improve the accuracy in port diameters.

Since it is difficult to decrease the dimension error below 0.01 mm, we have to increase the inner diameter of each port to decrease the error. For example, the O/F error decreases from 20% to 10% by increasing the port diameter from 0.3 mm to 0.6 mm. However, the increase in port diameters causes larger port intervals, resulting in a longer initial transient period. Since the initial transient is a period for the exit end face to attain a steady state shape, an initial end face shape being close to the steady state shape can shorten this period. As a nearly steady state shape, we employed a tapered fuel in Test-05 and Test-06, as shown in Fig. 13. A length of the tapered region of around 7.5 mm was determined from the results shown in Fig. 9; the initial transition period ends when the axial regression distance reaches 7 to 8 mm. Figure 14 shows a pressure history obtained with the tapered fuel (Test-05), along with the pressure history of Test-04 shown in Fig. 5. Both pressures are normalized by each mean value in a steady state period, 6.5 to 9.5 s for the straight port case (Test-04) and 1 to 3.5 s for the tapered port case (Test-05). The history

clearly shows that a steady state was attained in less than one second in the tapered port case. Figure 15 shows the O/F history for the straight and tapered port cases. Errors are not included in this figure to make it more readable. Again, O/F reaches a steady value within one second, showing that employing a fuel with a steady state shape has the benefit of shortened initial transient period.

IV. Conclusion

The recent technical progress of 3D printers made it possible to test the idea of end-burning type hybrid rockets experimentally. Employing an ultraviolet curable resin as a solid fuel, the authors made a verification firing of an end-burning type hybrid motor successfully for the first time. The results clearly show the initial transient and the steady periods of the end-burning mode. It also proves a virtue of no O/F shift during firing.

Another virtue of the end burning type hybrid rocket is the remarkable throttling characteristic; O/F shows almost no variation during throttling. Because of insufficient accuracies in port diameters, firing tests with various oxidizer flow rate showed no clear trend on the effect of oxidizer flow rate on O/F. To demonstrate the remarkable throttling characteristics more clearly, we have to improve the accuracy in port diameters.

Since the initial transient is a period for the exit end face to attain a steady state shape, an initial end face shape being close to the steady state shape can shorten this period. A firing test with a fuel having tapered ports showed that a steady state is attained in less than 1 second, which is much shorter than for the non-tapered case of about 6 seconds.

Acknowledgments

This work is supported by JSPS KAKENHI Grant Number 15K14243. The authors thank members of the Hybrid Rocket Research Working Group of Institute of Space and Astronautical Science, Japan Aerospace Exploration Agency, for their helpful discussion.

References

[1] Nagata, H., Aikawa, N., Akiba, R., Kudo, I., Ito, K., Tanatsugu, N., “Combustion Characteristics of Propellants for Dry Towel Hybrid Rocket Motor,” *48th International Astronautical Congress*, IAF-97-S.2.08, Torino, Italy, 1997.

[2] Nagata, H., Okada, K., San'da, T., Kato, T., Akiba, R., Satori, S., Kudo, I., “Combustion Characteristics of Fibrous Fuels for Dry Towel Hybrid Rocket Motor,” *Journal of Space Technology and Science*, Vol. 13, No.1, 1997, pp. 1_11-1_16.

doi: 10.11230/jsts.13.1_11

[3] Kato, T., Hashimoto, N., Nagata, H., Akiba, R., Kudo, I., "A preliminary study of End-Burning Hybrid Rocket, Part 1: Combustion Stability," *Journal of the Japan Society for Aeronautical and Space Science* (in Japanese), Vol. 49, No. 565, 2001, pp. 33-39.
doi: 10.2322/jjsass.49.33

[4] Hashimoto, N., Kato, T., Nagata, H., Akiba, R., Kudo, I., "A preliminary study of End-Burning Hybrid Rocket, Part 2: Combustion Characteristics," *Journal of the Japan Society for Aeronautical and Space Science* (in Japanese), Vol. 49, No. 565, 2001, pp. 40-47.
doi: 10.2322/jjsass.49.40

[5] Hashimoto, N., End-burning type hybrid rocket, Doctor thesis (in Japanese), Hokkaido University, 2004, Section 3.4, pp. 48-62.

[6] Hashimoto, N., Watanabe, S., Nagata, H., Totani, T., Kudo, I., "Opposed-flow flame spread in a circular duct of a solid fuel: Influence of channel height on spread rate," *Proceedings of the Combustion Institute*, Vol. 29, No. 1, 2002, pp. 245-250.
doi: 10.1016/S1540-7489(02)80033-5

[7] Hashimoto, N., Nagata, H., Totani, T., Kudo, I., "Determining Factor for the Blowoff Limit of a Flame Spreading in an Opposed Turbulent Flow in a Narrow Solid-fuel Duct," *Combustion and Flame*, Vol. 147, Issue 3, 2006, pp. 222-232.
doi:10.1016/j.combustflame.2006.07.015

[8]Matsuoka, T., Murakami, S., Nagata, H., "Transition characteristics of combustion modes for flame spread in solid fuel tube," *Combustion and Flame*, Vol. 159, No. 7, 2012, pp. 2466-2473.
doi:10.1016/j.actaastro.2010.07.009

[9] Xintian Li, Hui Tian, Nanjia Yu, and Guobiao Cai. "Experimental Investigation of Combustion in Axial-Injection End-Burning Hybrid Rocket Motor," *Journal of Propulsion and Power*, Vol. 31, No. 3, 2015, pp. 930-936.
doi:10.1016/j.actaastro.2016.02.023

[10] H. Nagata, H. Nakayama, M. Watanabe, M. Wakita, T. Totani, "Accuracy and applicable range of a reconstruction technique for hybrid rockets," *Advances in Aircraft and Spacecraft Science*, Vol. 1, No. 3, pp. 273-289, 2014.
doi: 10.12989/aas.2014.1.3.273

Table 1 Summary of Test Conditions.

Test	Burning duration [s]	Oxygen flow rate [g/s]	Chamber Pressure* [MPa]	Fuel consumption [g]	Initial port exit shape
01	6.4	0.38	0.19	4.42	Straight
02	6.1	0.96	0.49	7.28	Straight
03	10.2	0.49	0.24	4.55	Straight
04	9.7	0.45	0.23	5.28	Straight
05	3.7	0.95	0.47	3.83	Tapered
06	3.7	0.74	0.32	3.53	Tapered

*Average value during steady state region

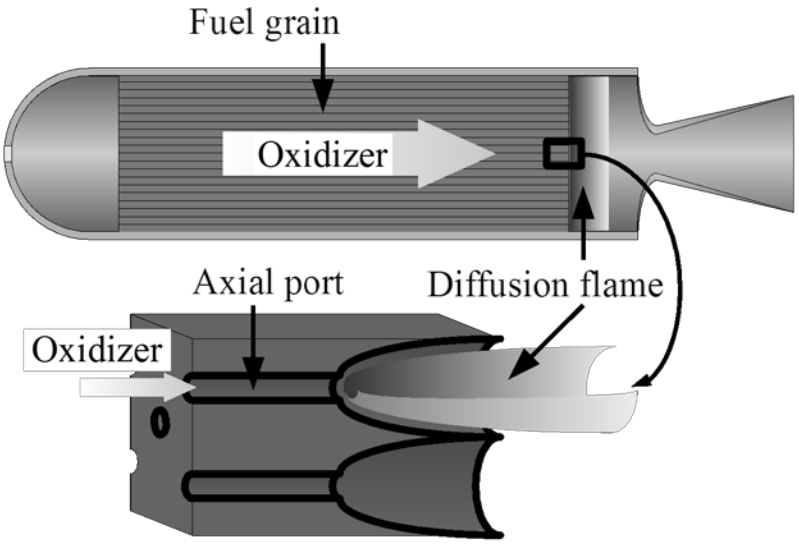

Fig. 1 Schematic concept of an end burning type hybrid rocket.

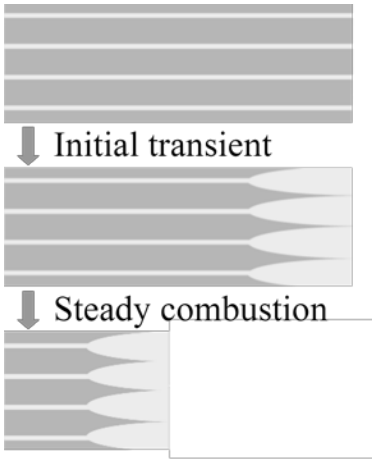

Fig. 2 Schematic image of the initial transient.

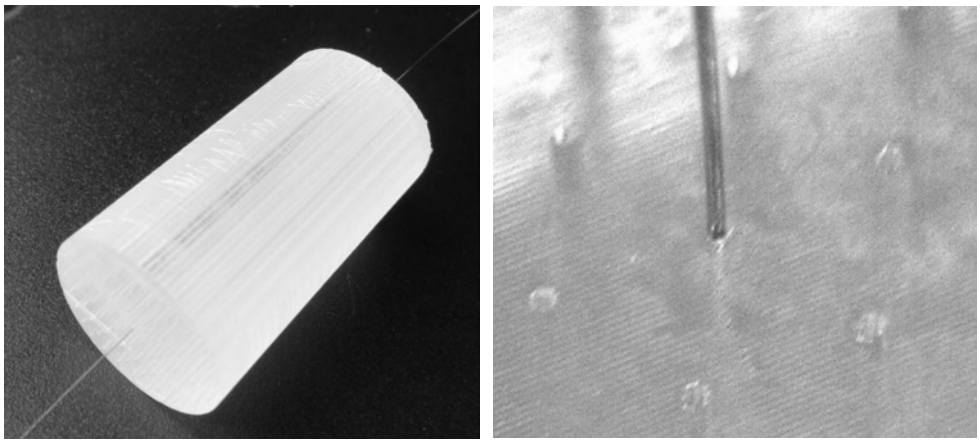

Fig. 3 Fuel grain.

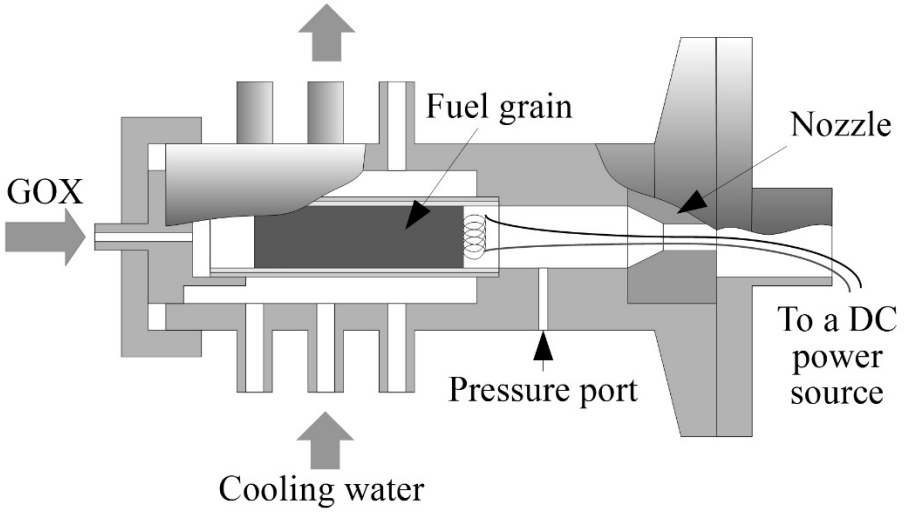

Fig. 4 Test motor.

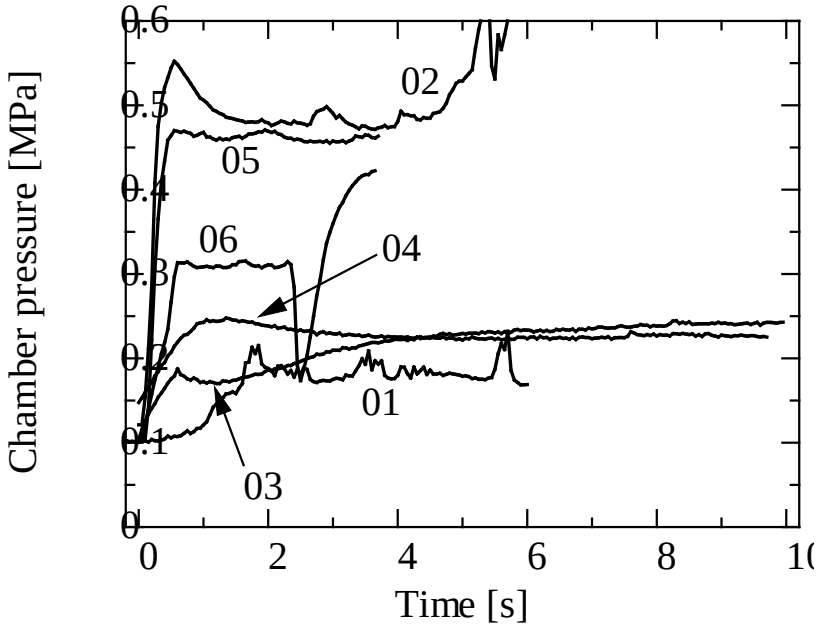

Fig. 5 Chamber pressure histories.

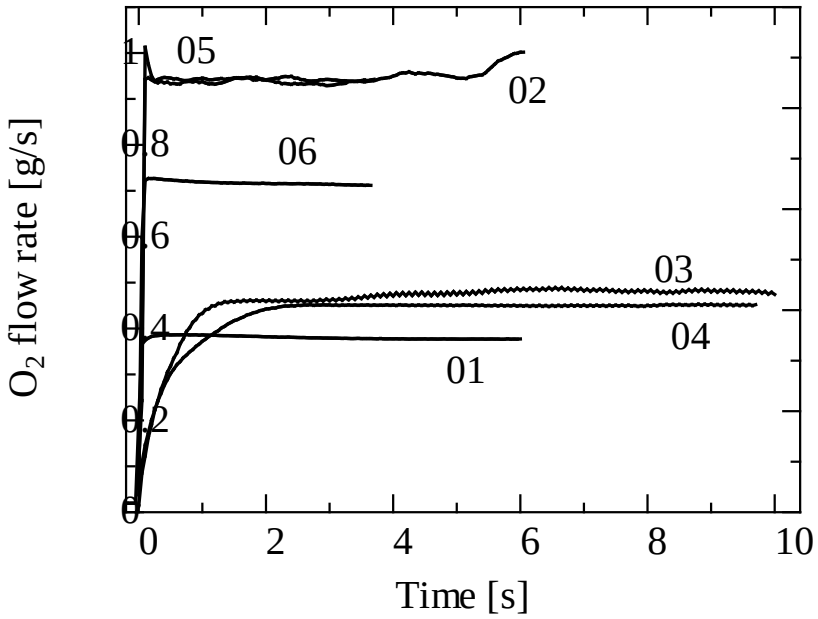

Fig. 6 Oxygen flow rate histories.

Fig. 7 Fuel grain after firing.

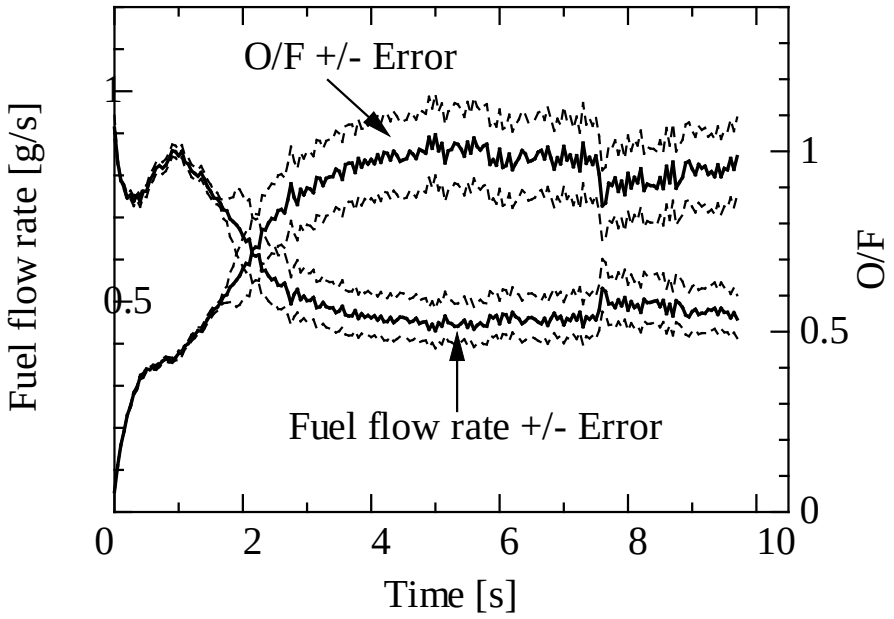

Fig. 8 Histories of chamber pressure and oxygen flow rate in Test-04.

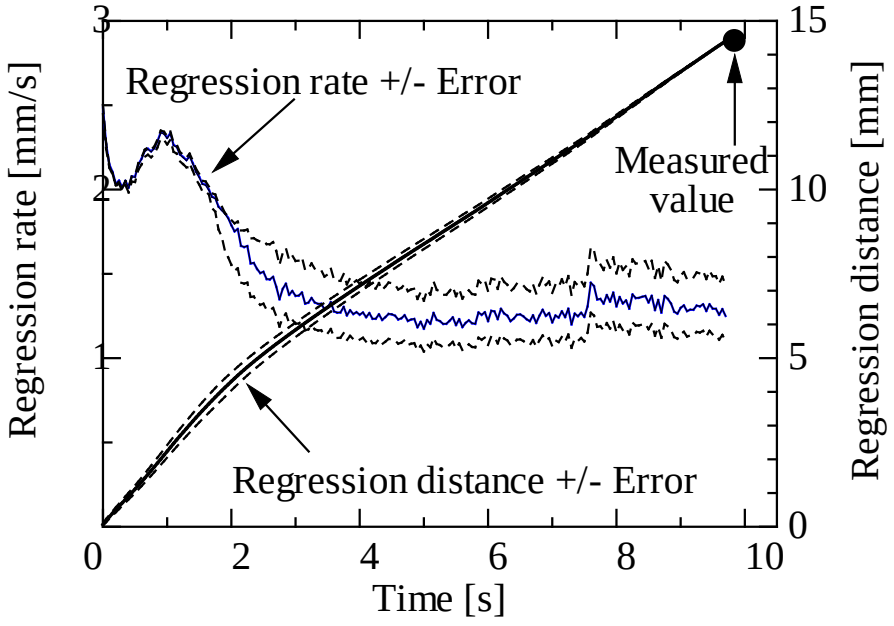

Fig. 9 Histories of axial regression rate and regression distance in Test-04.

Fig. 10 Radial vs. axial regression distances in each port.

Fig. 11 Duration of the initial transient in Test-04.

Fig. 12 Effect of oxidizer flow rate on oxidizer to fuel ratio.

Fig. 13 Dimensions of exits of a tapered fuel.

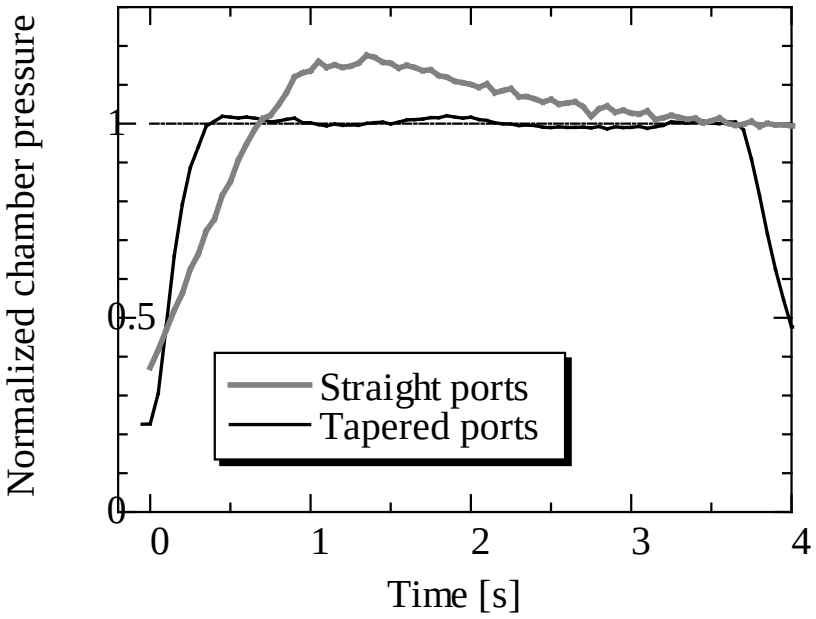

Fig. 14 Chamber pressure histories obtained by straight and tapered port fuels.

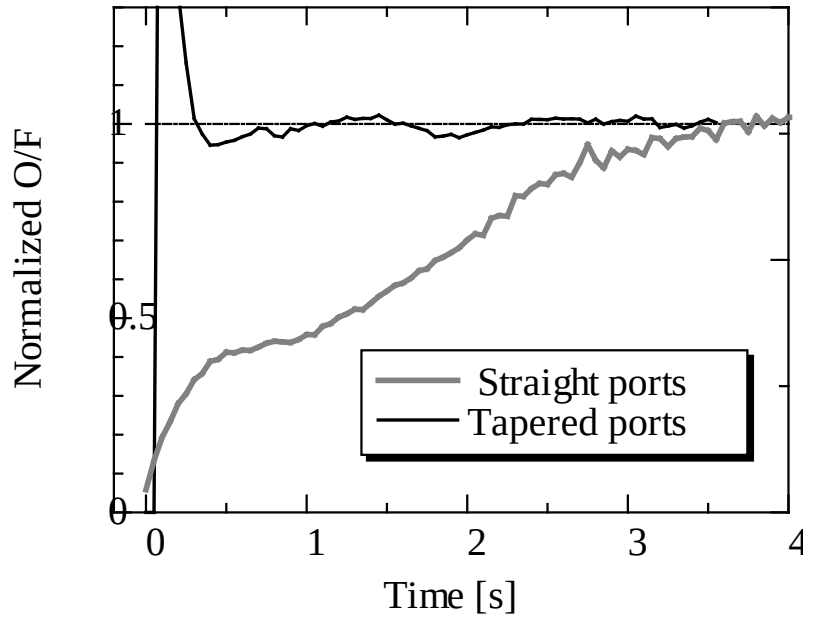

Fig. 15 O/F histories obtained by straight and tapered port fuels.